Pediatr Radiol (1991) 21: 211–215

Pediatric Radiology

MR-anatomy of infants hip: comparison to anatomical preparations

R. Krasny[1], A. Prescher[2], A. Botschek[1], R. Lemke[3], H.-R. Casser[4] and G. Adam[1]

[1] Department of Diagnostic Radiology, [2] Institute of Anatomy, [3] Institute of Forensic Medicine and
[4] Department of Orthopedic Surgery, University of Technology, Aachen, FRG

Received: 22 June 1990; accepted: 10 July 1990

Abstract. The correlation between anatomical preparations and MRI images of the most important structures of newborn hips in coronal and axial orientation was performed in 18 post mortem babies. T1-weighted images present a good differentiation between cartilage, bone, ligaments and surrounding soft tissues. Coronal images give the best opportunity to study the clinically important structures of the roof of acetabulum including the labrum and the ground of the acetabulum. The latter is shown in a more detailed way by MRI than by sonography. Axial images allow additional examinations of the ventral and dorsal parts of the joint. By using both coronal and axial images the exact determination of the centering of the femur head in the hip joint is possible.

Due to the excellent soft tissue contrast, MRI allows differentiation between bone marrow, cartilage, ligaments, fat pads, bursae and intraarticular fluid. MRI has proven itself useful in the examination of joints in a number of reports [1–3]. Reports concerning MR examination of infants' hips, however, are rare [4, 5].

The goal of the present study was to achieve a direct comparison of MR images and corresponding anatomical preparations of infants' hips in order to enable the localisation and identification of important structures composing and surrounding the hip joint.

Materials and methods

The hips of 18 post mortem infants aged between 3 weeks to 5.5 months were studied. The causes of death were not related to any kind of joint disorders, and the examinations were performed not later than within 40 h post mortem. Eight female and 10 male infants were examined.

MR images were obtained of the intact bodies as well as of the subsequent hemipelvectomy preparations in gelatin. We used a superconducting magnet with a field strength of 1.5 tesla (Magnetom, Siemens, FRG). According to the size of the examined object an appropriate surface coil (head-, spinal-, eye-ear coil and knee resonator) was used. All infants lay on their backs with extended slightly inwards rotated legs. The knee resonator was used only for the hemipelvectomy preparations. Bodies and hemipelvectomy preparations were positioned as carefully as possible in order to generate comparable images.

We used a T1-weighted spin-echo sequence (TR = 0.6 s, TE = 22 ms). Matrix 256 2, slice thickness of 3 mm with an interslice gap of 1 mm. Four acquisitions were taken. One of the two orthogonal planes (coronal or axial) was used in each child.

After the MRI examinations, hemipelvectomy preparations were obtained, deep frozen and cut into 4 mm planparallel slices

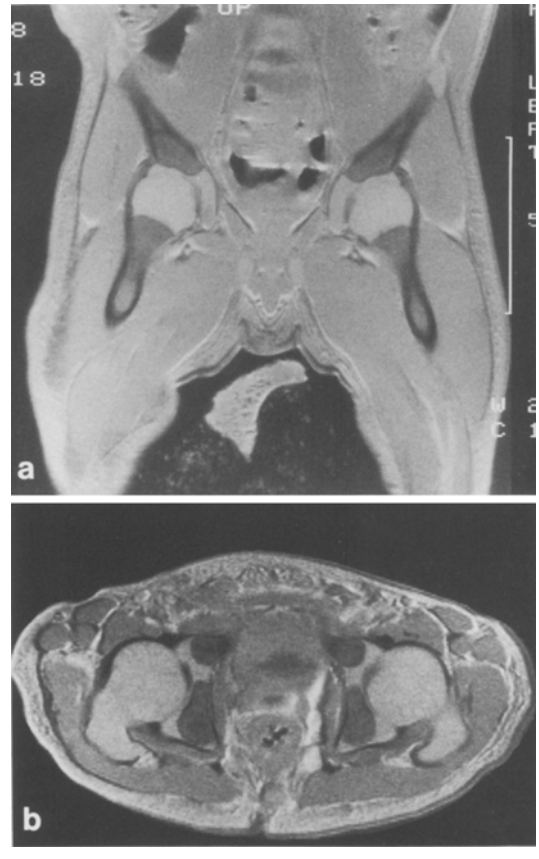

Fig. 1 a, b. MR-tomographic images of the infantal pelvis in coronal (**a**) and axial (**b**) slice orientation (Spin-echo 600/22)

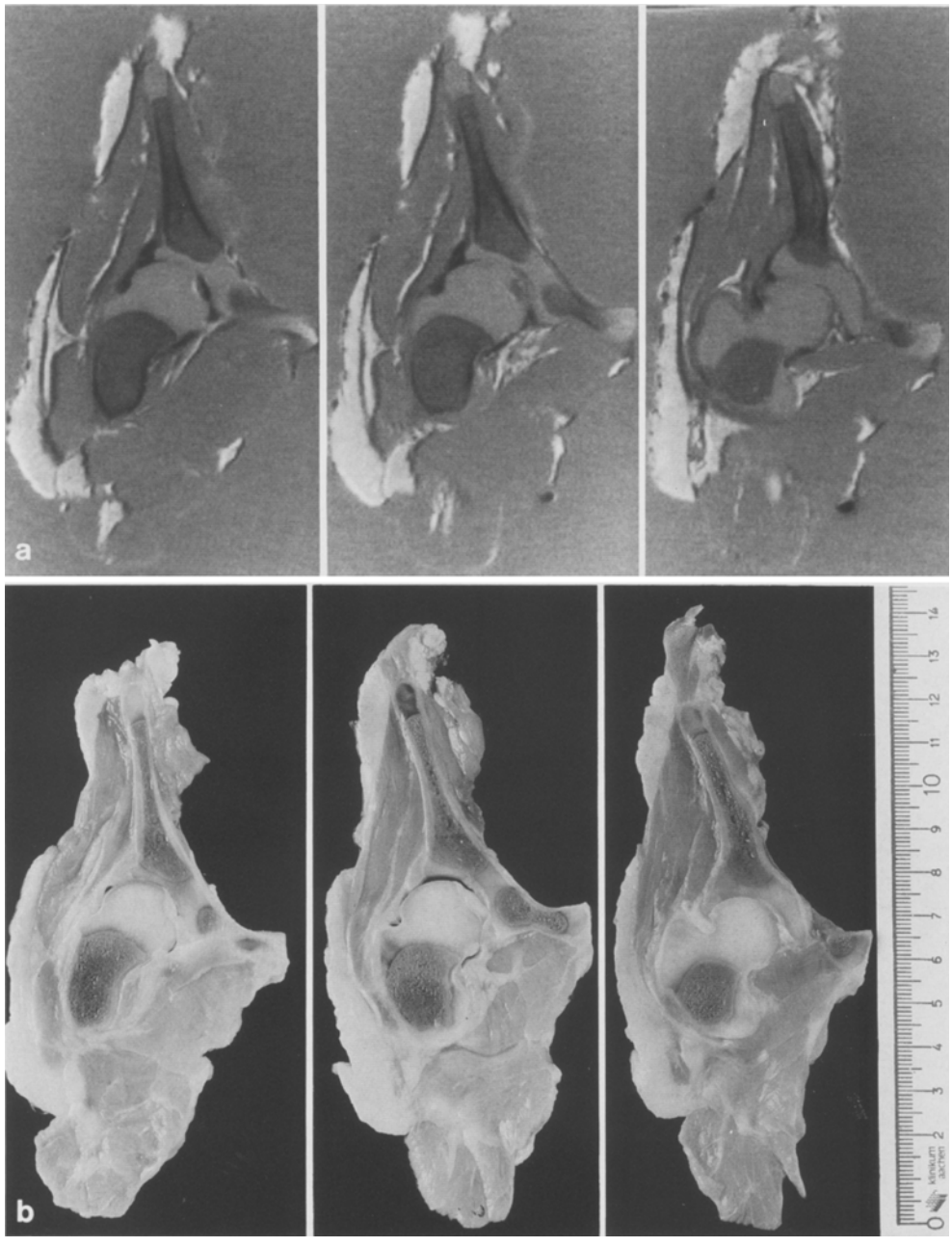

Fig. 2 a–c. MR images (**a**) of a preparation (**b**) of an infants hip joint in three different coronal positions (from ventral to dorsal, Spin-echo 600/22). The schematic drawing (**c**) explains the most important anatomical structures (▨ = bone; ▩ = hyaline cartilage; ■ = fibrous cartilage). For numbers see Table 1

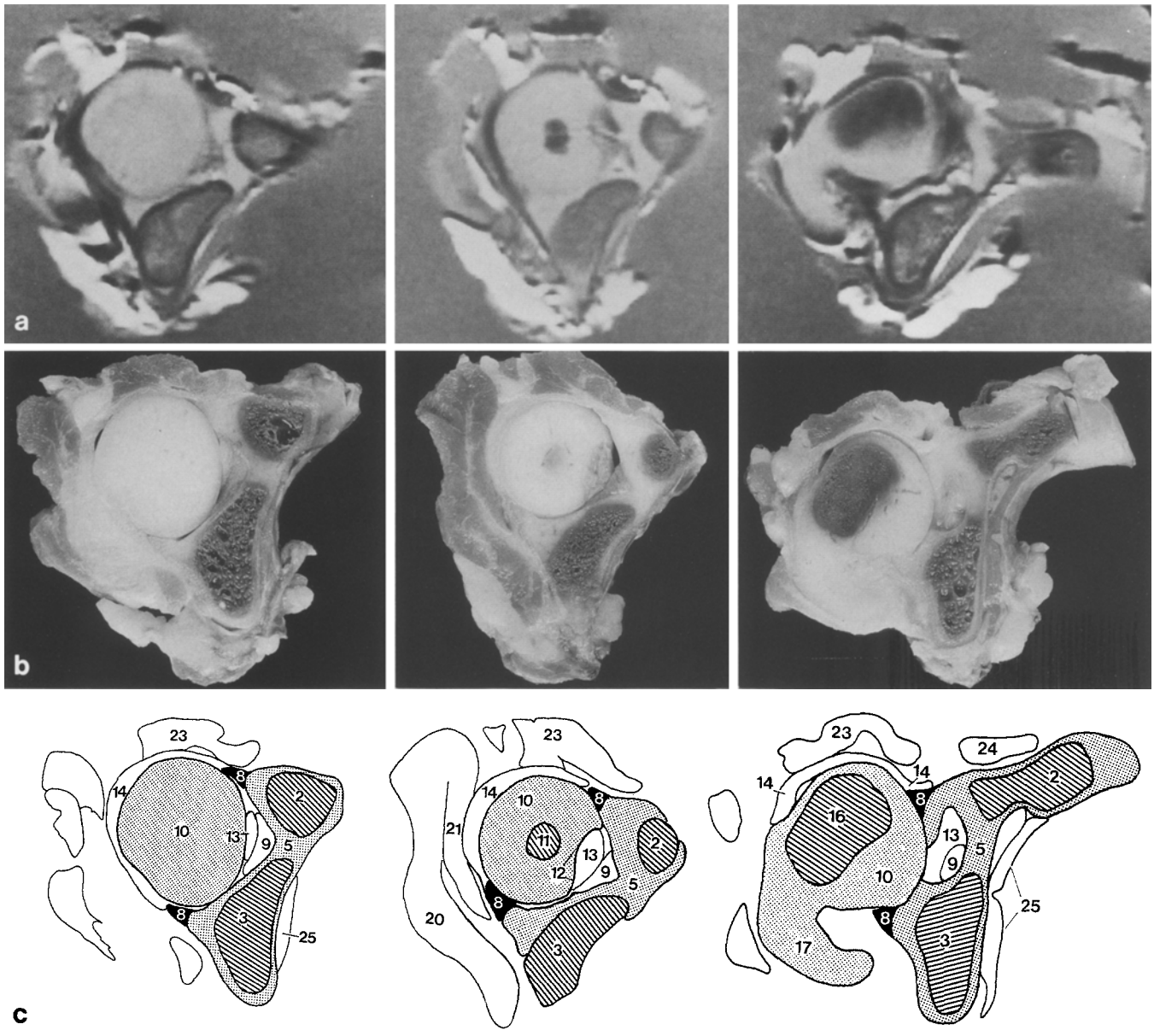

Fig. 3a–c. MR images (**a**) of a preparation (**b**) of an infants hip joint in three different axial positions (from cranial to caudal, Spin-echo 600/22). The schematic drawing (**c**) demonstrates the most imprortant anatomical structures (▨ = bone; ▩ = hyaline cartilage; ■ = fibrous cartilage). For numbers see Table 1

with a bone band saw. The slices were washed, dried and photographed as native preparations in black/white and in colour. Structures were identified and compared with those of MRI images.

Results

Coronar slice orientation (Figs. 1 a, 2)

The predominating structures of the infants' hip joint are the cartilaginous femoral head and the equally cartilagenous hip bone socket. The size and the contrast of hyaline cartilage to other structures in MRI lead to easy recognition of them in all slice orientations.

The bordering structures of the femoral head, as seen in coronal slice orientation, are recognized as follows: The epiphyseal cartilage towards caudal, the articular capsule towards mediocaudal and lateral and the joint cavity towards cranial and medial. The cartilaginous greater and lesser trochanter as well as the fovea capitis femoris may also be demonstrated in the respective images.

Three major parts of the hip socket can be discerned in coronal orientation, the roof of the acetabulum, the acetabular fossa and the triradiate cartilage. The acetabula fossa is viewed in a longitudinal orientation and imposes as a widening of the joint cavity. The contents of the acetabular fossa is mostly homogeneous in MRI. Neither the ligament of the femoral head nor the appropriate artery or vein can be identified. Only a small intraarticular fat pad (Pulvinar) is clearly delineated on its caudal rim.

Table 1. A list of the anatomical structures as seen in Figs. 2 and 3

(1)	ilium	(14)	articular capsule
(2)	pubis	(15)	zona orbicularis
(3)	ischium		
(4)	iliac crest	(16)	femur, diaphysis
		(17)	greater trochanter
(5)	triradiate cartilage	(18)	lesser trochanter
(6)	osseous protrusion		
(7)	cartilaginous protrusion	(19)	gluteus maximus muscle
(8)	labrum	(20)	gluteus medius muscle
(9)	pulvinar	(21)	gluteus minimus muscle
		(22)	iliacus muscle
(10)	femoral head	(23)	iliopsoas muscle
(11)	bony epiphysis	(24)	pectineus muscle
(12)	fovea capitis femoris	(25)	obturatorius internus
(13)	ligamentum teres		muscle

Depending on the slice position, one of the upper branches of the triradiate cartilage is intersected. A wide cartilaginous strip is then seen between the ilium bone and the pubic bone (ventrally) or the ischium bone (dorsally). The lower branch is cut longitudinally and seen in its full length.

Both, the bone and the cartilage structures of the acetabular roof, are seen best in coronar slice orientation. The thickness of the cartilage and its surface features can be well evaluated, as the joint cavity is visible in its entire length. The lateral portion of the roof of the acetabulum consists of the so-called cartilaginous and osseous protrusions. The osseous protrusions can appear either sharp-edged or rounded in coronal images, depending on positioning. The cartilaginous protrusions always appear rounded. The labrum acetabulare is situated, laterally, adjacent to the cartilaginous protrusion. It forms the circular rim of the acetabulum and has a triangular cross-section in the images. With the exception of the articular capsule, all neighbouring structures are easily differentiated. Both the articular capsule and the labrum acetabulare present good contrast to all bordering stuctures, both intraarticular and extraarticular. The zona orbicularis is not visible in MRI, even though it could be seen in anatomic specimens.

Axial slice orientation (Fig. 3)

Depending on the degree of anteversion, the femur head presents a comma-shaped protrusion in the dorso-lateral direction. This is caused by the greater trochanter. The epiphyseal cartilage cannot be seen in the joint images. The fovea capitis femoris is recognizable as a dent in the ventro-medial edge of the femur head.

The labrum acetabulare and the ventral and dorsal portions of the articular capsule can be evaluated in axial orientated images. The two upper branches of the triradiate cartilage are shown longitudinally in the appropriate slice images, the lower branch is seen in its cross-section. The acetabular fossa is dishshaped in these images. As in the coronar orientation, the ligament of the femur head can not be identified in MRI images.

Discussion

Conventional radiography is only able to demonstrate the osseous portions of the infant's hip. Arthrography allows only indirect evaluation of the cartilaginous femoral head and acetabulum. CT-images provide spatial, unobstructed views of the joint and surrounding soft tissue. Cartilage, however, is not directly visible with this technique [6–8]. Surrounding tissue offers indirect information concerning the joint cartilage. Furthermore, the high radiation dose involved with CT examinations limits its use on children [9].

Direct imaging of the cartilaginous structures of joints first became possible with the development of ultrasonic imaging. But even under optimal examination conditions, one cannot determine the complete contour and structure of cartilages. Especially the caudal and medial portions of the joint are not sufficiently visible. Small structures, such as the articular cavity or the ligament of the femoral head cannot be evaluated due to the small spacial resolution [10–12].

MRI represents an important progress in the examination of hips. Without applying contrast medium or radiation, it is possible to achieve high-resolution, multiplanar images and a brilliant soft tissue contrast. As proven in the present study, MRI allows simultaneously imaging of cartilage, the synovial fluid, the ligaments, the articular capsule, fat pads, muscle, vessels, subcutaneous fat and skin.

Preliminary clinical experience demonstrate the good visibility of effusion in T2 weighted images (Fig. 4a). Using fast- sequence images with gradient echo pulse sequences even cartilage-effusion-contrast is enhanced and a clear differentiation of the other joint-structures is

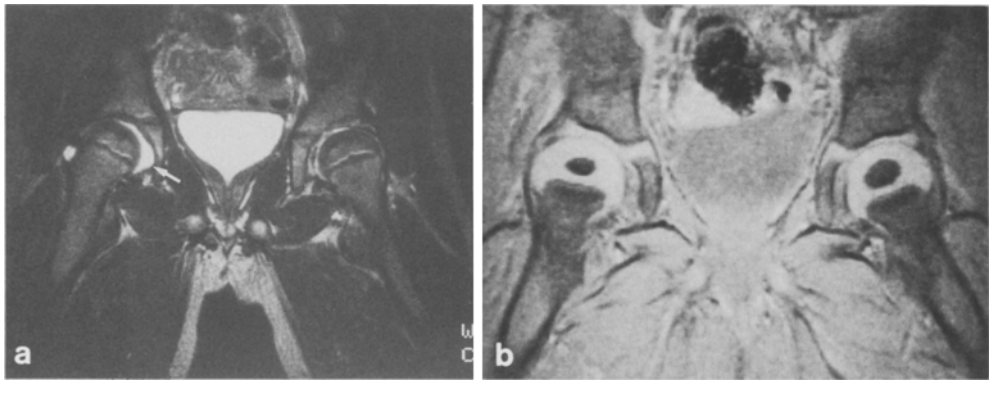

Fig. 4. a Four and half years old child with successful treated congenital dislocation on both sides. In T2-weighted Spin-Echo image (200/90) clearly evidence of effusion (→) on the right hip. **b** One year old child with mild congenital dislocation on both sides. Under use of Gradient-Echo-Sequence FLASH 0.07/10 with an Flip angle of 30 with good differentiation of all important structures of the hip

possible Fig. 4b). Furthermore, the examination time is remarkably reduced by these fast imaging sequences.

Coronal slices are valuable, as this orientation delivers anatomical images which are known in plain radiography and ultrasound. Additional orientations, especially axial images increase the examiner's spatial orientation and improve the diagnostic abilities concerning the ventral and dorsal joint regions.

References

1. Adam G, Bohndorf K, Prescher A, Krasny R, Günther RW (1988) Der hyaline Gelenkknorpel in der MR-Tomographie des Kniegelenkes bei 1.5 T. Fortschr Röntgenstr 148: 648–651
2. Hajek PC (1987) MR arthrography: anatomic pathologic investigation. Radiology 163: 141–147
3. Middleton WD (1987) High resolution surface coil magnetic resonance imaging of the joints: anatomic correlation. Radiographics 7: 645
4. Johnson ND (1988) Complex infantile and congenital hip dislocation: Assessment with MR Imaging. Radiology 168: 151–156
5. Johnson ND, Wood BP, Noh KS, Jackman KV, Westersson P-L, Katzberg RW (1989) MR imaging anatomy of the infant hip. AJR 153: 127–133
6. Hernandez RJ (1985) CT evaluation of pediatric hip disorders. Orthop Clin N Am 16: 513
7. Lingg G (1983) Zur Wertigkeit der Computertomographie bei kongenitalen Hüftdysplasie und Hüpftluxation. Röntgen-Blätter 36: 407–413
8. Lafferty CM (1986) Acetabular alteration in untreated congenital dysplasia of the hip: computed tomography with multiplanar re-formation and three-dimensional analysis. J Comput Assist Tomogr 10: 84–91
9. Stargardt A, Gursky S, Rockstroh G (1984) Zum Strahlenrisiko der Computertomographie. Radiol Diagn 25: 205–212
10. Pfeil J (1986) Darstellung des neonatalen Hüftgelenkes in der anatomischen Frontalebene und im Ultraschallbild. Z Orthopädie. 124: 188–191
11. Casser H-R, Forst R (1985) Realtime-Sonographie des kindlichen Hüftgelenkes zur Frühdiagnostik der kongenitalen Hüftdysplasie. Klin Pädiatr 197: 398–408
12. Graf R (1981) The ultrasonic image of the acetabular rim in infants. Arch Orthop Trauma Surg 99: 35–41

Dr. R. Krasny
Department of Diagnostic Radiology
University of Technology Aachen
Pauwelsstraße 30
W-5100 Aachen
FRG

Literature in pediatric radiology (continued from p. 210)

Measurement of progressive cerebral ventriculomegaly in infants after grades III and IV intraventricular hemorrhages. Brann IV, B.S. et al. (Dept. of Ped., Children's Hosp., Univ. School of Med., 2211 Lomas Blvd., Albuquerque, NM 87131, USA) **117,** 615 (1990)

Ectopic pregnancy in adolescents: a clinical review for pediatricians. Ammerman, S. et al. (Shafer, M-A., Div. of Adolescent Med., Univ., 400 Parnassus Av., Room A-268, San Francisco, CA 94143, USA) **117,** 677 (1990)

Serial magnetic resonance imaging in neonatal hypoxic-ischemic encephalopathy. Byrne, P. et al. (3A3, Walter MacKenzie Health Science Centre, Univ. Edmonton, Alberta, T6G 2G4, Canada) **117,** 694 (1990)

Clinicopathologic review of twelve children with nephropathy, Wilms tumor, and genital abnormalities (Drash syndrome). Jadresic, L. et al. (Dept. of Paed. Nephrol., Inst. of Child Health, 30 Guilford St., London WC1N 1EH, UK) **117,** 717 (1990)

Journal of Pediatric Surgery (New York)

Delayed presentation of Hirschsprung's disease: acute obstruction secondary to megacolon with transverse colonic volvulus. Neilson, I.R., Youssef, S. (Youssef, S., Dept. of Ped. Surg., Children's Hosp., McGill Univ., 2300 Tupper St., Montreal, Quebec H3H 1P3, Canada) **25,** 1177 (1990)

Journal of Urology (Baltimore)

Pheochromocytoma in the pediatric age group: the prostate- an unusual location. Voges, G.E. et al. (Dept. of Urol., Univ. Med. School, W-6500 Mainz, FRG) **144,** 1219 (1990)

Medical and Pediatric Oncology (New York)

Effect of abdominal irradiation on growth in boys treated for a Wilm's tumor. Wallace, W.H.B. et al. (Shalet, S.M., Dept. of Endocrinol., Christie Hosp., Wilmslow Rd., Withington, Manchester M20 9BX, England) **18,** 441 (1990)

Superior vena cava syndrome associated with childhood malignancy: analysis of 24 cases. Ingram, L. et al. (Shapiro, D.N., St. Jude Children's Research Hosp., 332 N. Lauderdale, Memphis, TN 38105, USA) **18,** 476 (1990)

Pediatric Cardiology (New York)

Noninvasive assessment of coarctation of the aorta: comparative measurements by two-dimensional echocardiography, magnetic resonance, and angiography, Stern, H.C. et al. (Dept. of Ped. Cardiol., Deutsches Herzzentrum, Lothstr. 11, W-8000 München 2, FRG) **12,** 1, (1991)

Percutaneous transluminal coronary angioplasty for Kawasaki disease: a case report and literature review. Ino, T. et al. (Dept. of Ped., Juntendo Univ. School of Med., 2-1-1 Hongo, Bunkyou-ku, Tokyo 113, Japan) **12,** 33 (1991)

Aberrant left pulmonary artery with tracheal stenosis without vascular sling. Moreno, F. et al. (Hosp. Infantil La Paz, Paseo de la Castellana, 261, E-28046 Madrid, Spain) **12,** 44 (1991)

Intrapericardial teratoma causing nonimmune hydrops fetalis and pericardial tamponade: a case report. Rheuban, K.S. et al. (Dept. of Ped., Box 386, Univ. of Health Sciences Center, Charlottesville, VA 22908, USA) **12,** 54 (1991)

Pediatrics (Evanston IL)

Periventricular-intraventricular hemorrhage sonographic localization, phenobarbital, and motor abnormalities in low birth weight infants. Krishnamoorthy, K.S. et al. (Ped. Neurol Unit, General Hosp., Fruit St., Boston, MA 02114, USA) **85,** 1027 (1990)

Real-time ultrasound and color-Doppler imaging in pulmonary sequestration. Newman, B. (Dept. of Rad., Univ. School of Med. and Children's Hosp., Pittsburgh, PA, USA) **86,** 620 (1990)

Radiology (Easton PA)

Extremity osteosarcomas: intraarterial chemotherapy and limb-sparing resection with 2-year follow-up. Kashdan, B.J. et al. (Sullivan, K.L., Dept. of Rad., Jefferson Med. College and Thomas Jefferson Univ. Hosp., 111 S 11th St., 5609 New Hosp., Philadelphia, PA 19107, USA) **177,** 95 (1900)

Usefulness of a short femur in the in utero detection of skeletal dysplasias. Kurtz, A.B. et al. (Dept. of Rad., Div. of Diagn. Ulrasound, Jefferson Med. College and Thomas Jefferson Univ. Hosp., Main Bldg., Seventh Floor, 111 S 11th St., Philadelphia, PA 19107, USA) **177,** 197 (1990)

Conjoined twins: prenatal diagnosis and assessment of associated malformations. Barth, R.A. et al. (Dept. of Rad., Section of Diagn. Ultrasound, Univ., Med. Center Hosp., 111 Colchester Av., Burlington, VT 05401, USA) **177,** 201 (1990)

Cloacal malformations and exstrophy syndromes. Wood, B.P. (Dept. of Rad., Childrens Hosp., 4650 Sunset Blvd., Los Angeles, CA 90054-0700, USA) **177,** 326 (1990)

Development of the human cerebellum observed with high-field-strength MR imaging. Stricker, T. et al. (Dept. of Ped., Univ, Hosp., 5841 S Maryland Av., Box 455, Chicago, IL 60637, USA) **177,** 431 (1990)

Phenylketonuria: MR imaging of the brain with clinical correlation. Pearsen, K.D. et al. (65 Caversham Woods, Rochester, NY 14534, USA) **177,** 437 (1990)

The cloacal malformation: radiologic findings and imaging recommendations. Jaramillo, D. et al. (Lebowitz, R.L., Dept. of Rad., Children's Hosp., Harvard Med. School, 300 Longwood Ave., Boston, MA 02115, USA) **177,** 441 (1990)

(continued on p. 233)